Void Reactivity Decomposition Analysis for LWR Fuel Assembly having MOX and FCM rods

Dae Hee Hwang and Ser Gi Hong[*]
Department of Nuclear Engineering, Kyung Hee University
1732 Deogyeong-daero, Giheung-gu, Yongin-si, Gyeonggi-do, 17104, Republic of Korea
[*]*Corresponding author: sergihong@khu.ac.kr*

1. Introduction

Recently, the deep-burning of TRU (Transuranics) nuclides from PWR spent fuel without recycling and their multi-recycling using PWR have been studied as alternative ways for the direct geological disposal. In particular, the authors recently have suggested the multi-recycling of TRU nuclides in a specialized PWR fuel assemblies comprised of MOX and FCM fuels [1]. In this concept, the TRU nuclides are recycled through the MOX fuel rods while the TRUs produced from FCM ones are not recycled due to their deep burning. From view point of neutronics, one of the most important issues is the positive void reactivity which can occur in a PWR fuel assembly containing TRU nuclides [2].

The purpose of this work is to give the physical understanding of the void reactivity in the specialized PWR fuel assemblies having MOX and FCM fuel rods with the reactivity decomposition method. Specifically, we applied a method using normalization to total integral flux for the reactivity decomposition analysis based on the neutron balance equation.

2. Methods and Results

In this study, DeCART2D (Deterministic Core Analysis based on Ray Tracing for 2-Dimensional core) code was used for analyzing the fuel assembly level calculations [3]. DeCART2D code has been developed at KAERI (Korea Atomic Energy Research Institute) to generate few group homogenized neutron cross section data. DeCART2D code solves the multi-group transport equation by using MOC (Method of Characteristics).

A reactivity decomposition method was suggested by the second author for better understanding of the sodium void reactivity in SFR (Sodium cooled Fast Reactor) based on the neutron balance equation [4, 5]. This decomposition method was devised by decomposing the reactivity change into the leakage, capture, fission, and (n, 2n) contributions and it uses the normalization of these contributions to one neutron produced by fission (i.e., normalization to the production rate). This method gives the exact reactivity change, but it has a disadvantage that it does not explain the change in the fission production rate. Sun et al., suggested alternative normalization to the total integral flux (i.e., the integrated flux over all energy groups and volume) and they also applied these methods to understand the sodium void reactivity in SFR cores [6]. In these

decomposition methods, it is assumed that the each parameter of leakage, capture, fission, and production rate is independent variable. This assumption was found to be quite accurate. In this work, the leakage term can be neglected because the fuel assembly calculation was performed with reflective boundary condition. The leakage rate in PWR is not as large as in the fast reactor. Thus, the reactivity change $\Delta\rho$ can be expressed as:

$$\Delta\rho = (\frac{\partial\rho}{\partial c})_N \Delta c + (\frac{\partial\rho}{\partial f})_N \Delta f + (\frac{\partial\rho}{\partial p})_N \Delta p, \qquad (1)$$

where c, f, p represent the capture, fission, and production rate, respectively and N indicates a nominal state. In Eq. (1), the (n, 2n) and (n, 3n) reaction are neglected due to their small contribution in thermal spectrum. The final expression for the void reactivity decomposition can be expressed as [6]:

$$\Delta\rho = -\frac{c_V - c_N}{p_N} - \frac{f_V - f_N}{p_N} + \frac{p_V - p_N}{p_N k_{eff,N}} \qquad (2)$$

$$= \sum_i C_i + \sum_i F_i + \sum_i P_i, \qquad (3)$$

where V indicates a voided state. In this work, all of the reaction rates in Eq. (2) were normalized to total integral flux. In Eq. (3), C_i, F_i, and P_i represent the nuclide-wise contributions by capture, fission and fission production, respectively, that are given by:

$$C_i = -\frac{c_{V,i} - c_{N,i}}{p_N},$$

$$F_i = -\frac{f_{V,i} - f_{N,i}}{p_N},$$

$$P_i = \frac{p_{V,i} - p_{N,i}}{p_N k_{eff,N}},$$

Where $c_{V,i}$, $f_{V,i}$ and $p_{V,i}$ represent the capture, fission, and fission production rate, respectively, of nuclide i over the fuel assembly.

2.1 Fuel Assembly Design

The reference fuel assembly has 17×17 rod array and it is composed of 212 MOX rods, and 52 FCM TRISO rods. Table I summarizes the design specification of the fuel assemblies. The case of B0 is non-recycled FA in which the MOX rods are composed of 90.19 wt% UO_2 (4.95 wt% enrichment), 7.31 wt% $TRUO_2$ and 2.5 wt% Mo. A small addition of Mo into MOX pellets was considered to enhance an accident tolerance such as the

improvements of the thermal conductivity and the FP retention capability of the fuel pellets [7]. In this work, three different TRU compositions in MOX fuels are considered to reflect the effect of TRU recycling on the coolant void reactivity. The first case (i.e., B0) represents the fresh composition without TRU recycling (i.e., BOC of the first cycle). That is to say, the TRU compositions in MOX and FCM fuel rods are the one of the PWR spent fuel TRU having 50 MWD/kg and 10 years cooling. The TRU compositions of the second and third cases are extracted from the one of twice and five times recycled TRUs. That is to say, the TRU composition of the second case is the one of the twice burnt fuel with recycling. In this work, all the fission products are removed during reprocessing and enriched UO_2 is supplied to make up these fission products' removal. With this kind of recycling scheme, TRU content in MOX fuel decreases as recycling and so the second and third cases have lower TRU contents in MOX fuels. In addition, the recycling of TRU reduces the fissile content in TRU.

Table I: Design specification of the reference fuel assemblies

Parameter	FA ID (the number of recycling)		
	B0 (0)	H0 (2)	S0 (5)
Rod array	17×17		
Pellet radius (cm)	0.4095		
Clad. Thickness (cm)	0.0655		
Rod diameter (cm)	0.95		
Clad. material	Zircaloy-4		
Pin pitch (cm)	1.2234		
Assembly pitch (cm)	20.879		
P/D ratio	1.288		
MOX rod			
The number of rods	212		
Pellet material	4.95 wt% enriched UO_2 -7.31 wt% $TRUO_2$ -2.50 wt% Mo	4.95 wt% enriched UO_2 -6.38 wt% $TRUO_2$ -2.50 wt% Mo	4.95 wt% enriched UO_2 -5.87 wt% $TRUO_2$ -2.50 wt% Mo
Densigy (g/cm³)	10.392		
FCM TRISO rod			
The number of rods	52		
Kernel material	$TRUO_2$		
Density (g/cm³)	10.430		
Kernel diameter (μm)	800		
Buffer thickness (μm)	80		
IPyC thickness (μm)	20		
SiC thickness (μm)	35		
OPyC thickness (μm)	20		
Packing fraction (%)	40		

Fig. 1 compares k-inf at BOC as a function of void fraction for the typical UO_2 fuel assembly (FA) and the special FAs having MOX and FCM fuels. In case of the typical UO_2 FA, the k-inf monotonically decreases as void fraction increases, while for the special FAs considered in this work, the k-infs decrease as the void fraction increases up to ~70 % and hereafter the k-infs increases as void fraction increases. Especially, in case

of B0, the k-inf at 99 % void fraction was evaluated higher than that at nominal state (i.e., 0 % void fraction) because of its high TRU content. The monotonic decrease of k-inf for the typical UO_2 FA means that this FA has negative void reactivity coefficient. On the other hand, the positive slopes of k-inf curves for the special FAs mean that they have positive void reactivity coefficient at the high void fractions at which the positive slopes occur.
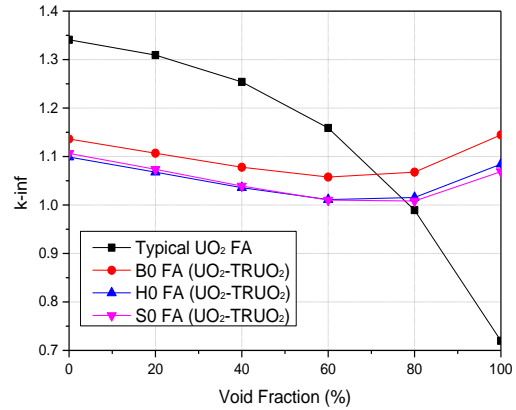

Fig. 1. Comparison of k-inf at BOC as a function of void fraction

Fig. 2 shows the normalized neutron spectra for typical UO_2 FA and B0 FA with various void fractions. As shown in the figure, it is noted that the thermal peak around 0.1 eV shown in the case of UO_2_VF0 almost disappears for the special FAs and the neutron spectra were significantly hardened. This is because TRU nuclides have considerably high thermal absorption cross section. The neutron spectra were gradually more hardened as the void fraction increases. Actually, this spectrum hardening leads to the increase of neutron leakage which induces a large negative reactivity contribution for large void fraction at which a positive void reactivity occurs. This leakage effect is not considered in the fuel assembly level with reflective boundary condition.
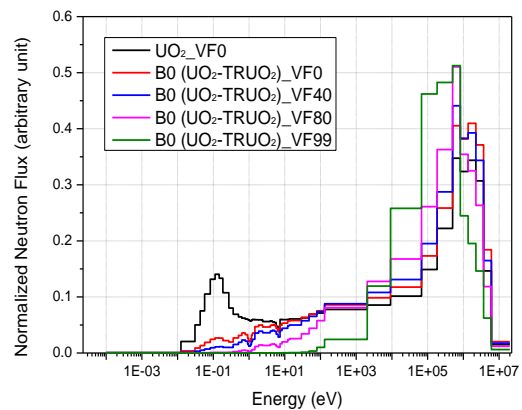

Fig. 2. Comparison of normalized neutron spectra for typical UO_2 FA and B0 FA with various void fractions

2.2 Decomposition Analysis results

In this section, the reactivity decomposition method with total integral flux normalization is applied for better understanding of the void reactivity coefficient. We considered three different voiding levels (i.e., 0 %, 40 %, and 80 % voiding) and 1 % additional voiding at these voiding levels to model the void reactivity coefficients. The results (i.e., nuclide-wise and reaction-wise contributions) of the decomposition of void reactivity caused by 1 % additional voiding are given in Table II. They are also graphically shown in Fig. 3 and Fig. 4. In Table II, it is noted that the capture and fission contributions to the reactivity caused by 1 % additional voiding are positive while the contributions from fission production are negative at the all of the three voiding levels for all the nuclides. That is to say, the spectrum hardening resulted from voiding reduces the one-group capture and fission cross sections (i.e., effective capture and fission rates) but increases the fission production one. For the 1 % additional voiding at no voiding state, the total capture and fission contributions are 304 and 289 pcm, respectively. The summations of these positive fission and capture contributions are smaller than the negative one from fission production, which gives a negative void reactivity of 77 pcm. As the voiding level increases, the positive contributions from capture and fission increase. In particular, the positive contribution from capture more rapidly increases than the fission and the negative fission production contributions. For the 1 % additional voiding at the 40 % voiding level, the void reactivity is still negative

due to a large negative contribution from fission production. On the other hand, the void reactivity for the 1 % additional voiding at the 80 % voiding level is estimated to be positive (148.5 pcm) due to large positive contributions from capture and fission. In Table II, the total reactivities obtained with the decomposition method are compared with those obtained with the nominal voiding level and 1 % additional voided state k-infs. Table II shows that the decomposition method gives nearly the same reactivity as the one calculated with k-infs at the nominal and 1 % additional voided state. In Fig. 3, it is noted that all three FAs have similar levels of void reactivity and trends versus nominal voiding level even if they have different TRU compositions. Actually, these trends are due to the fact that TRU contents in MOX fuels decrease as recycling in our recycling scheme.

When comparing each nuclide, it was notable that U-235, Pu-239, Pu-241, Am-242m, Cm-243, and Cm-245 contributed to a negative reactivity for all of void fraction ranges, and the remaining nuclides such as U-238, Np-237, Pu-238, Pu-240, Pu-242, Am-241, Am-243, Cm-242, Cm-244, and Cm-247 contributed to a positive reactivity. As shown in Fig. 4, Pu-239 had the largest negative reactivity contribution due to fission production reaction, followed by those of U-235 and Pu-241. On the other hand, Pu-240 had largest positive reactivity contribution by capture reaction in the voiding level range of 0-80%, and U-238 had largest positive reactivity in the voiding level larger than 80 %. The reduction of capture reaction in the structure also contributed to a positive reactivity.

Table II: Nuclide-wise reactivity contributions for each reaction for B0 FA

(a) 0-1 % void fraction (direct $\Delta\rho$ = -77.5 pcm)

| Nuclide	0 % VF			1 % VF			ΔC_i	ΔF_i	ΔP_i	Sum
(i)	C_i	F_i	P_i	C_i	F_i	P_i	(pcm)	(pcm)	(pcm)	(pcm)
U-235	1.04E-03	2.92E-03	7.14E-03	1.04E-03	2.90E-03	7.09E-03	21.3	66.4	-153.5	-65.9
U-238	3.92E-03	6.02E-04	1.68E-03	3.91E-03	6.01E-04	1.68E-03	25.4	2.5	-5.5	22.4
Np-237	7.26E-04	2.84E-05	8.39E-05	7.23E-04	2.84E-05	8.38E-05	9.8	0.0	-0.1	9.7
Pu-238	9.19E-05	2.88E-05	8.87E-05	9.13E-05	2.88E-05	8.87E-05	2.0	0.0	-0.1	2.0
Pu-239	2.97E-03	5.33E-03	1.54E-02	2.95E-03	5.28E-03	1.52E-02	95.2	175.6	-442.9	-172.0
Pu-240	2.68E-03	7.56E-05	2.38E-04	2.66E-03	7.56E-05	2.37E-04	67.6	0.1	-0.3	67.3
Pu-241	4.99E-04	1.51E-03	4.46E-03	4.95E-04	1.50E-03	4.43E-03	14.6	40.4	-99.4	-44.4
Pu-242	4.89E-04	2.39E-05	7.63E-05	4.87E-04	2.39E-05	7.63E-05	7.3	0.0	-0.1	7.3
Am-241	1.37E-03	3.20E-05	1.08E-04	1.36E-03	3.20E-05	1.08E-04	32.9	0.2	-0.6	32.6
Am-242m	2.03E-06	1.10E-05	3.61E-05	2.00E-06	1.09E-05	3.56E-05	0.1	0.5	-1.4	-0.8
Am-243	3.41E-04	5.55E-06	1.99E-05	3.39E-04	5.54E-06	1.99E-05	5.2	0.0	-0.1	5.1
Cm-242	1.26E-09	4.05E-10	1.48E-09	1.26E-09	4.04E-10	1.48E-09	0.0	0.0	-0.0	0.0
Cm-243	1.69E-07	1.20E-06	4.12E-06	1.68E-07	1.19E-06	4.10E-06	0.0	0.0	-0.1	-0.0
Cm-244	3.53E-05	2.85E-06	9.30E-06	3.52E-05	2.85E-06	9.30E-06	0.3	0.0	-0.0	0.3
Cm-245	7.73E-07	5.36E-06	1.93E-05	7.67E-07	5.32E-06	1.92E-05	0.0	0.1	-0.4	-0.3
Cm-246	7.78E-08	1.71E-08	5.63E-08	7.77E-08	1.71E-08	5.63E-08	0.0	0.0	-0.0	0.0
Structure	1.06E-03	0.00E+00	0.00E+00	1.06E-03	0.00E+00	0.00E+00	22.4	0.0	0.0	22.4
Total	1.52E-02	1.06E-02	2.93E-02	1.51E-02	1.05E-02	2.91E-02	304.1	288.7	-669.8	-77.0

(b) 40-41 % void fraction (direct $\Delta\rho$ = -108.8 pcm)

Nuclide	40 % VF			41 % VF			ΔC_i	ΔF_i	ΔP_i	Sum
(i)	C_i	F_i	P_i	C_i	F_i	P_i	(pcm)	(pcm)	(pcm)	(pcm)
U-235	8.38E-04	2.07E-03	5.07E-03	8.32E-04	2.05E-03	5.02E-03	29.7	105.0	-242.9	-108.2
U-238	3.48E-03	5.53E-04	1.54E-03	3.47E-03	5.51E-04	1.54E-03	82.4	8.4	-24.0	66.7
Np-237	5.71E-04	2.73E-05	8.03E-05	5.67E-04	2.73E-05	8.01E-05	23.3	0.2	-0.6	22.9
Pu-238	6.79E-05	2.80E-05	8.59E-05	6.73E-05	2.79E-05	8.57E-05	3.0	0.1	-0.5	2.6

Pu-239	1.83E-03	3.26E-03	9.42E-03	1.80E-03	3.21E-03	9.28E-03	135.7	264.2	-681.4	-281.4
Pu-240	1.74E-03	7.28E-05	2.28E-04	1.71E-03	7.27E-05	2.27E-04	139.5	0.5	-1.7	138.3
Pu-241	3.22E-04	1.02E-03	3.01E-03	3.17E-04	1.01E-03	2.97E-03	22.5	62.7	-166.4	-81.3
Pu-242	3.68E-04	2.29E-05	7.28E-05	3.64E-04	2.28E-05	7.26E-05	20.6	0.2	-0.7	20.1
Am-241	9.20E-04	2.84E-05	9.60E-05	9.07E-04	2.83E-05	9.56E-05	63.9	0.6	-1.8	62.7
Am-242m	1.01E-06	5.70E-06	1.87E-05	9.89E-07	5.57E-06	1.83E-05	0.1	0.6	-1.9	-1.1
Am-243	2.59E-04	5.16E-06	1.85E-05	2.56E-04	5.14E-06	1.84E-05	13.8	0.1	-0.2	13.6
Cm-242	1.16E-09	3.88E-10	1.41E-09	1.16E-09	3.87E-10	1.41E-09	0.0	0.0	-0.0	0.0
Cm-243	1.27E-07	9.17E-07	3.16E-06	1.26E-07	9.09E-07	3.13E-06	0.0	0.0	-0.1	-0.1
Cm-244	2.96E-05	2.72E-06	8.85E-06	2.94E-05	2.71E-06	8.83E-06	0.9	0.0	-0.1	0.9
Cm-245	5.19E-07	3.65E-06	1.32E-05	5.16E-07	3.61E-06	1.30E-05	0.0	0.2	-0.7	-0.5
Cm-246	7.01E-08	1.62E-08	5.33E-08	6.98E-08	1.62E-08	5.32E-08	0.0	0.0	-0.0	0.0
Structure	7.26E-04	0.00E+00	0.00E+00	7.16E-04	0.00E+00	0.00E+00	54.0	0.0	0.0	54.0
Total	1.12E-02	7.10E-03	1.97E-02	1.10E-02	7.02E-03	1.94E-02	589.7	423.1	-1120.3	-107.5

(c) 80-81 % void fraction (direct $\Delta\rho$ = 152.1 pcm)

| Nuclide	80 % VF			81 % VF			ΔC_i (pcm)	ΔF_i (pcm)	ΔP_i (pcm)	Sum (pcm)
(i)	C_i	F_i	P_i	C_i	F_i	P_i				
U-235	5.10E-04	1.19E-03	2.93E-03	4.96E-04	1.17E-03	2.87E-03	129.8	251.2	-596.3	-215.3
U-238	2.50E-03	4.26E-04	1.18E-03	2.46E-03	4.20E-04	1.17E-03	394.8	57.0	-151.5	300.3
Np-237	3.05E-04	2.38E-05	6.94E-05	2.96E-04	2.36E-05	6.88E-05	90.4	1.8	-5.1	87.1
Pu-238	4.11E-05	2.60E-05	7.93E-05	4.02E-05	2.59E-05	7.89E-05	8.8	1.2	-3.6	6.4
Pu-239	7.53E-04	1.42E-03	4.13E-03	7.28E-04	1.38E-03	4.01E-03	246.4	400.9	-1077.0	-429.7
Pu-240	5.25E-04	6.41E-05	1.99E-04	4.96E-04	6.36E-05	1.97E-04	292.3	4.4	-13.5	283.1
Pu-241	1.38E-04	5.01E-04	1.48E-03	1.33E-04	4.86E-04	1.44E-03	49.8	141.1	-392.6	-201.7
Pu-242	1.47E-04	1.97E-05	6.23E-05	1.40E-04	1.95E-05	6.17E-05	69.3	1.6	-5.0	65.9
Am-241	3.56E-04	2.13E-05	7.23E-05	3.42E-04	2.10E-05	7.14E-05	144.3	2.8	-8.9	138.2
Am-242m	2.58E-07	1.57E-06	5.16E-06	2.45E-07	1.49E-06	4.91E-06	0.1	0.7	-2.3	-1.4
Am-243	1.09E-04	4.12E-06	1.47E-05	1.04E-04	4.07E-06	1.46E-05	47.0	0.5	-1.6	45.8
Cm-242	8.46E-10	3.40E-10	1.23E-09	8.30E-10	3.37E-10	1.22E-09	0.0	0.0	-0.0	0.0
Cm-243	6.01E-08	4.39E-07	1.51E-06	5.78E-08	4.22E-07	1.46E-06	0.0	0.2	-0.5	-0.3
Cm-244	1.51E-05	2.31E-06	7.49E-06	1.45E-05	2.29E-06	7.42E-06	5.8	0.2	-0.6	5.4
Cm-245	2.55E-07	1.75E-06	6.31E-06	2.48E-07	1.69E-06	6.12E-06	0.1	0.5	-1.8	-1.2
Cm-246	4.69E-08	1.35E-08	4.43E-08	4.58E-08	1.34E-08	4.39E-08	0.0	0.0	-0.0	0.0
Structure	4.85E-04	0.00E+00	0.00E+00	4.78E-04	0.00E+00	0.00E+00	63.3	0.0	0.0	63.3
Total	5.89E-03	3.70E-03	1.02E-02	5.73E-03	3.62E-03	1.00E-02	1542.3	850.3	-2244.1	148.5
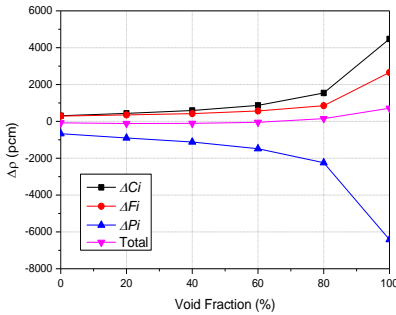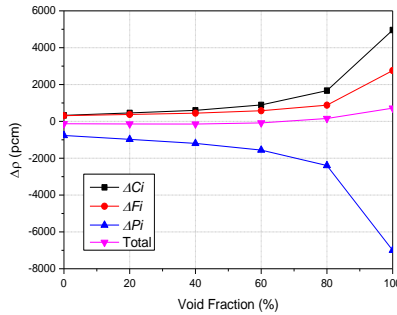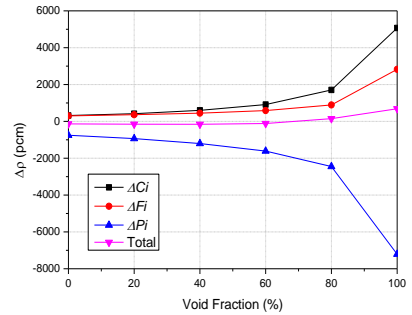
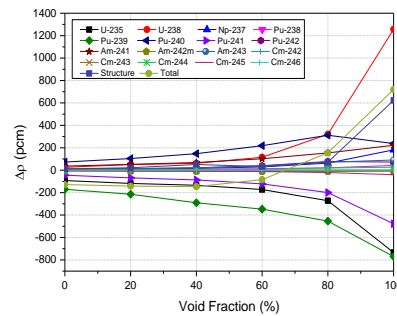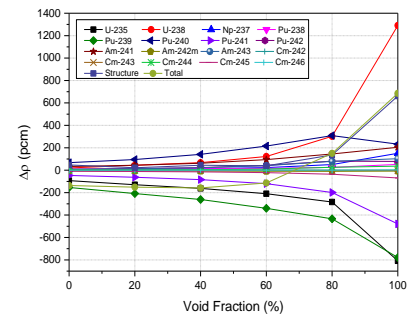(a) B0 FA (non-recycled) (b) H0 FA (twice-recycled) (c) S0 FA (five times-recycled)

Fig. 3. Reactivity change by each reaction term for three FAs with different number of recycling
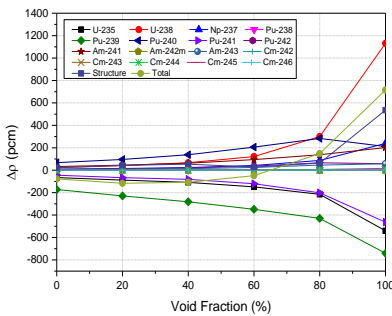
(a) B0 FA (non-recycled) (b) H0 FA (twice-recycled) (c) S0 FA (five times-recycled)

Fig. 4. Reactivity change by each nuclide for three FAs with different number of recycling

3. Conclusions

In this study, the reactivity decomposition analysis for LWR FAs composed of MOX rods and FCM rods were performed to analyze the effect of each nuclide to void reactivity. In particular, three different FAs having different TRU contents and compositions were considered to show the effect of TRU recycling on the void reactivity. The void reactivity was decomposed with normalization to total integral flux into nuclide-wise contributions for each reaction type. From the decomposition analysis, it was shown that 1) the decomposition method gives the almost exact reactivity within about 3.6 pcm displacement bound compared to the direct reactivity change calculated with nominal and voided states, 2) the positive contribution to the void reactivity comes from the reactions in capture and fission (in particular, capture contribution is much larger than the fission one) for high nominal voiding levels, and 3) the plutonium isotopes having even mass number, Np-237, Am-241, and Am-243 give much positive contributions while the negative contributions come from the fissile nuclides due to the reaction in the fission production under voiding.

ACKNOWLEDGEMENT

REFERENCES

[1] D. H. Hwang, J. Y. Choi, and S. G. Hong, "TRU transmutation in Light Water Cooled SMR cores loaded with Fuel Assemblies composed of MOX and FCM fuel rods," Transactions of the Korean Nuclear Society Autumn Meeting Gyeongju, Korea, October 26-27, 2017.
[2] Y. S. Cho, D. H. Hwang, and S. G. Hong, "A Neutronic Study of TRU Multi-recycling in MOX and FCM Fueled PWR Assemblies," PHYSOR 2018, Cancun, Mexico, April 22-26, 2018.
[3] J. Y. Cho et al., "DeCART2D v.1.0 User's Manual," KAERI/TR-5116/2013, Korea Atomic Energy Research Institute, 2013.
[4] S. G. Hong, S. J. Kim, and Y. I. Kim, "Annular Fast Reactor Cores with Low Sodium Void Worth for TRU Baring," Nuclear Technology, Vol. 162, 1-25 (2008).
[5] S. G. Hong et al., "Neutronic Characterization of Sodium-cooled Fast Reactor in an MHR-SFR synergy for TRU Transmutation," Proceedings of ICAPP2007, Nice, France, May 13-18, 2007.
[6] K. Sun et al., "Void reactivity decomposition for the Sodium-cooled Fast Reactor in equilibrium fuel cycle," Annals of Nuclear Energy 38 (2011) 1646-1657.
[7] D. J. Kim et al., "Fabrication of Micro-cell UO_2-Mo Pellet with Enhanced Thermal Conductivity," Journal of Nuclear Materials 462 (2015) 289-295.